Design of an Advanced Distributed Adaptive Control for Multi-SMA Actuators

Belkacem Kada*, Khalid A. Juhany, Ibraheem Al-Qadi, Mostefa Bourchak
Aerospace Engineering Department, King Abdulaziz University, Jeddah, KSA

***Abstract*—Aerospace applications place high demands on designing Shape Memory Alloy (SMA) actuators, including accuracy, dependability, high-performance criteria, and cooperative activation. Because of their portability, durability, and performance under extreme conditions, SMAs have found a home in the aerospace industry as single and array actuators. This paper presents the development of a control scheme for thermally activating rotary SMA actuators as single and cooperative actuators. The control scheme is a hybrid adaptive robust control abbreviated as HARC. The immersion and invariance adaptive (I&I adaptive) and L2-gain control frameworks are utilized in developing the HARC approach. To create stable transient responses despite parametric and non-parametric errors, recursive backstepping is utilized for asymptotic stability. At the same time, L2-gain control is applied to ensure the global stability of the transient closed-loop system. Both techniques are used in conjunction with one another. In contrast to the conventional I&I, the robust control law can be developed without needing a target system or the solution of PDEs to satisfy the I&I condition. The parametric uncertainty is estimated with the help of an adaptive rule, and the non-parametric uncertainty brought on by the phase change of the SMA material and modeling mistakes is accounted for with the help of asymptotic nonlinear functions. The designed HARC is then extended to cover the actuation of multi-SMA or array actuators to respond to the increasing demand for cooperative controllers using distributed control protocols. It has been demonstrated through simulation testing on a rotational NiTi SMA actuator that the suggested control approach is both practical and resilient.**

***Keywords*—Adaptive backstepping; hysteresis; I&I control; L_2-gain control; rotary actuator; shape memory alloy**

I. Introduction

Shape memory alloy (SMA) materials are promising materials for enhanced aircraft actuation because to their excellent physical and thermomechanical properties. SMA materials outperform other materials in terms of shape memory effect (SME) and superelasticity. The capacity of distorted SMA to regain its original shape following heating is referred to as superelasticity. Because of their superior performance qualities, SMA actuators can be employed in place of more traditional actuation solutions like solenoids, motors, thermometers, and even vacuum and pneumatic systems. SMA actuators have excellent control characteristics such as rapid response time, oscillation damping, and low power consumption. SMA actuators are of tremendous interest and usage in many cutting-edge industries, such as aerospace, automotive, information technology, and biomedical engineering [1-3]. Additionally, SMA actuators are highly effective at absorbing and dissipating mechanical energy. They can be used in numerous forms, including wires, springs, and strips. Typically, the actuation frequency of SMA actuators is much lower than that of conventional actuators such as DC/AC motors and hydraulic systems.

SMA twist or rotational actuators are a feasible solution for traditional step motors. They can be used to make helical torsion springs, twisted wires, twisted strips, thin-sheet torsional actuators, and antagonistic multiple-wire designs [4,5]. Applications for SMA torsional actuators include self-reconfigurable and modular robots, surgical instruments, and transformable wings [6-8]. SMA thermal activation via Joule heating with an electrical current is an efficient way for optimizing the effect of shape memory [9,10]. Understanding the heat activation and heat transport mechanisms of shape memory alloys is essential for employing them creatively and increasing their possible uses. However, the solid-state phase transformation and its accompanying physical phenomena, such as hysteresis, make regulating SMA-based actuators a difficult task.

To address the problem of SMA twist actuator control, various nonlinear control approaches were used. Sliding mode control (SMC) has been used in a variety of topologies to address nonlinear dynamics and hysteresis in SMA materials, as well as parameter uncertainties in system modeling. A wide range of SMC-based rotary SMA controllers have been designed and implemented for a wide range of engineering systems, including morphing airplanes [11], artificial muscles inspired by the human arm [12], multi-rod bars for flexible robotic arms [13], and flexible needles for clinical applications [14]. Despite applying various strategies, such as the saturation boundary layer function, the SMC-based controllers displayed control input chattering, which is damaging to the actuation systems. The challenges of SMA modeling and control have been overcome, for example, by employing fuzzy logic control (FLC) and artificial neural networks (AINN). Several studies on FLC and ANN for SMA have been published [15-20]. However, both FLC and ANN implementation necessitate sophisticated and time-consuming techniques.

Adaptive backstepping control (ABC) is a powerful robust control approach that is commonly used in the control design of nonlinear, dynamically unpredictable, and nonsmoothed systems. ABC is a promising new method for industrial applications, particularly in electrical, medical, and aerospace systems. Few studies have been conducted to address the problem of SMA hysteresis control using nonlinear adaptive backstepping control. Recently, [21] addressed the problem of hysteresis in control systems by employing a unique hysteresis

model and an ABC to assure stable and accurate control. In [22], authors used ABC to design a control system for a soft robotic muscle inspired by biology. The authors demonstrated that ABC outperforms adaptive sliding mode control regarding time-domain response performance. This paper presents a new hybrid adaptive robust control (HARC) method to thermally activate SMA rotary actuators in the presence of parametric and non-parametric uncertainties. The technique combines I&I-adaptive control with L_2-gain control. A Lyapunov-based analysis of the controller's stability is presented. The proposed controller can provide robust and rapid tracking of the desired system response despite its asymptotic convergence. The following is the outline for the paper. In Section II, the thermomechanical modeling of a rotary SMA actuator is presented along with the control objective of this paper. Section III presents the design of a nonlinear backstepping controller and an adaptive parameter law. Additionally, a stability analysis is investigated. Section IV presents numerical results, while Section V provides a conclusion and future perspectives.

II. Mathematical Modeling of a Rotary SMA Actuator and Control Objective

In this study, the angular position response of a rotary SMA actuator is controlled by the thermally induced shape-memory effect (SME) under electrical current input where the electrical power is converted to heat. Typically, this mechanism is used to control the SMA actuator. Under the influence of heat, the SMA actuator phase transitions from martensite to austenite and then back to martensite upon cooling. Fig. 1 shows some aerospace applications of SMA actuators.

a)

b)

Fig. 1. SMA actuators applied in aerospace control i: a) SMA actuator for Boeing 777-300ER airplane engines [24]; b) SMA actuator for torque control of the outboard wing section.

A heating or cooling process governs the phase transformation of SMAs from martensite to austenite and vice versa. During the heating process, unloaded martensite begins to transform into austenite at the austenitic start temperature A_s with a martensite volume fraction $\xi = 1$. The transformation continues until the austenitic transition temperature A_f and $\xi = 0$ are reached. The hysteresis loop depicted in Fig. 1(b) explains the irreversible nature of the crystalline structure change during thermally induced SME.

A. Thermomechanical Modeling

Consider an SMA model wire with a small diameter and a lumped capacitance, where the internal thermal gradient is small and the latent heat effects are negligible. The following lumped-capacitance thermal and Liang-Brinson phenomenological model was found to be adequate for this study [24].

$$\begin{cases} mC_p\dot{T} + hA_c[T - T_0] = R\,u \\ \dot{\sigma} = E\dot{\epsilon} + \Omega\dot{\xi} + \Theta\dot{T} \end{cases} \tag{1}$$

where, σ, ϵ, T denote the stress, strain, and temperature states; m,C_p,h,A_c, R denote the actuator's mass, specific heat, convection heat transfer coefficient, convection area, and resistor, respectively; Ω denotes the phase transformation, T_{amb} is the ambient temperature and $u = i_c^2$ denotes the control input where i_c is the electrical current. The elastic deformation ϵ is given by

$$\epsilon = (l - l_0 - r\theta)/l_0 \tag{2}$$

where, l_0 is the initial length of the SMA actuator. The lumped-capacitance thermal model exhibits mathematically simple behavior and conforms to Newton's law of cooling.

$$T_{cool}(t) = T_0 + (T_w - T_0)e^{-\lambda t} \tag{3}$$

where, T_0 is the ambient temperature, T_w is the initial temperature of the wire, and $\lambda = hA_c/mC_p$. The stress-strain model is a macro-mechanical or phenomenological constitutive law developed by Tanaka and updated by Liang and Brinson [25]. The model considers both thermomechanical and phase transformations. In Liang-Brinson model, the phase transformation volume fraction is modified to include the effect of complex loadings using cosine function rather than the exponential function used in Tanaka model.

B. Enhanced SME Model

We use the Elahinia-Ahmadian phase transformation model to predict the SMA behavior under complex fast stress and temperature loadings, which is the case for most rotary actuators. Experiments have demonstrated that the modified model can predict SMA behavior under complex loading conditions [26, 27]. The martensite volume fraction is calculated using the following equation during the reverse transformation of martensite to austenite by heating.

$$\xi = \frac{\xi_M}{2}\{cos[a_A(T - A_s) + b_A\sigma] + 1\} \tag{4}$$

The reverse phase transformation occurs under the following heating and unloading conditions.

$$\begin{cases} A_s + \frac{\sigma}{C_A} < T < A_f + \frac{\sigma}{C_A} \\ \dot{T} - \frac{\dot{\sigma}}{C_A} > 0 \end{cases} \quad (5)$$

Similar conditions were developed for the modified austenite to martensite phase transformation using cosine equation. The martensite volume fraction is computed as follows:

$$\xi = \frac{1-\xi_A}{2} cos\left[a_M\left(T - M_f\right) + b_M\sigma\right] + \frac{1+\xi_A}{2} \quad (6)$$

with

$$\begin{cases} M_f + \frac{\sigma}{C_M} < T < A_s + \frac{\sigma}{C_M} \\ \dot{T} - \frac{\dot{\sigma}}{C_M} < 0 \end{cases} \quad (7)$$

In this formulation C_M and C_A are material properties which describe the relationship between temperature and critical stress to induce transformation, and the parameters a_M and a_T are defined by

$$a_M = \frac{\pi}{M_S - M_f}, \qquad a_A = \frac{\pi}{A_f - A_S} \quad (8)$$

C. Kinematic and Dynamic Modeling

The SMA actuator model is a bias-type actuator whose general kinematics and dynamics equations are given as follows:

$$\begin{cases} \dot{\theta} = \omega \\ J\dot{\omega} + b(\theta)\omega + k\theta = \tau_s(\sigma) \end{cases} \quad (9)$$

where, θ, ω, J, b, k are the actuator's angular position, angular velocity, effective inertia, damping, and stiffness, respectively; τ, σ denote the control effort and the Piola-Kirchhoff's stress. The input torque $\tau_s(\sigma)$ is supposed to be a linear function of the mechanical stress σ

$$\tau(\sigma) = Ar\sigma \quad (10)$$

D. Control Objective

The control objective is to guarantee that the transient trajectories of the angular position, angular speed, the temperature are globally bound and converge to a new equilibrium despite hysteresis. We introduce, in systems (1) and (9), the new states $x_1 = \theta, x_2 = \omega, x_3 = T$ with an initial steady-state operating equilibrium defined as $[\theta_0 \quad \omega_0 \quad T_0]^T$

$$\begin{cases} \dot{x}_1 = x_2 \\ \dot{x}_2 = -a_1 x_1 - \beta x_2 + a_2 x_3 + f_1(\xi, T) \\ \dot{x}_3 = -b_1(x_3 - T_0) + b_2 u + f_2(\xi, T) \end{cases} \quad (11)$$

with

$$\begin{cases} a_1 = k/J, \ \ a_2 = \alpha\, Ar/J, \ \beta = b/J, \\ b_1 = hA_c/(mC_p), \ \ b_2 = R/(mC_p) \end{cases}$$

The model in (11) is a nonlinear dynamic model where β denotes the uncertainty in the damping properties of the actuator and $f_1(\xi)$ and $f_2(\dot{\xi})$ are uncertain bounded functions denoting the nonlinear hysteretic terms. The upper limits $f_1(\xi)$ and $f_2(\dot{\xi})$ satisfy

$$|f_i| \le l \in \mathbb{R}^+ \quad (12)$$

For simplicity, in the following $f_1(\xi)$ and $f_2(\xi)$ are substituted by f_1 and f_2. The control input u in (11) is designed to provide a robust and adaptive control input to the thermal actuation system of the SMA actuator. The adaptive law $\hat{u} = u(x, \hat{\beta})$, where $\hat{\beta}$ denotes the estimator of β provided by a proper adaptive law, is designed to compensate for parametric and non-parametric uncertainties. The robustness control component is designed using dissipation theory for which an energy storage function $V(\boldsymbol{x}(t))$ is selected to guarantee the following condition.

$$V(\boldsymbol{x}(t)) - V(\boldsymbol{x}(0)) = \int_0^T L(\boldsymbol{f}(\xi))dt \quad (13)$$

where $\boldsymbol{f} = [f_1 \quad f_2]^T$ and L is an energy supply function. The parameter adaptive law is designed as follows.

$$\dot{\hat{\beta}} = \Phi(\boldsymbol{x}, \hat{\beta}) \quad (14)$$

In absence of phase transformation, the control input $u(x, \hat{\beta})$ with the parameter adaptive law (14) guarantee the global asymptotic stability of the closed loop (11). For the case $f_i \neq 0$ $(i = 1,2)$, a global asymptotic stability is provided by the control law $u(x, \hat{\beta})$ under L_2-gain control bound.

III. Adaptive Robust SMA controller Design

A. Parameter Adaptive Law

The parameter adaptive law is designed to alleviate the influences of nonlinear parameter uncertainties. To construct the adaptive law (14), a parameter estimation error is defined as follows:

$$\varphi = \hat{\beta} - \beta + \rho(x_1, x_2) \quad (15)$$

where, $\rho(x_1, x_2)$ can be chosen as function of the actuator's motion states and be designed such that $\lim_{t\to\infty} \varphi = 0$. For simplicity $\rho(x_1, x_2)$ is denoted by ρ. The time derivative of expression (15) along the trajectories (11) gives

$$\dot{\varphi} = \dot{\hat{\beta}} + \frac{\partial \rho}{\partial x_1}\dot{x}_1 + \frac{\partial \rho}{\partial x_2}\dot{x}_2 \quad (16)$$

Using the dynamic model in (11), the time derivative $\dot{\varphi}$ is written as follows

$$\dot{\varphi} = \dot{\hat{\beta}} + \frac{\partial \rho}{\partial x_1}x_2 + \frac{\partial \rho}{\partial x_2}(-a_1 x_1 - \beta x_2 + a_2 x_3 + f_1) \quad (17)$$

Consider the case of $f_1 = 0$ and suppose that φ is asymptotically convergent function with $\lim_{t\to\infty} \varphi = 0$, the estimator $\dot{\hat{\beta}}$ can be chosen as

$$\dot{\hat{\beta}} = -\frac{\partial \rho}{\partial x_1}x_2 - \frac{\partial \rho}{\partial x_2}(-a_1 x_1 - (\hat{\beta} + \rho)x_2 + a_2 x_3) \quad (18)$$

which yields to

$$\dot{\varphi} = -\frac{\partial \rho}{\partial x_2}(\varphi x_2 - f_1) \quad (19)$$

B. Robust Control Law Design

To design a robust SMA controller, we define for the dynamic system the following tracking errors

$$\begin{cases} e_1 = x_1 - x_1^* \\ e_2 = x_2 - x_2^* \end{cases} \quad (20)$$

where, x_1^*, x_2^* are of class $C^{(0)}$ and define the desired states that serve as virtual control inputs to the first and second equations of model in (11).

Step 1: Angular position subdynamics stabilization

From the first equation in system in (20), the dynamic of e_1 is obtained as

$$\dot{e}_1 = x_2 = e_2 + x_2^* \quad (21)$$

With $e_2 = 0$, the system in (21) is stable under the following virtual control law.

$$x_2^* = -k_1 x_1 \quad (22)$$

Step 2: Angular velocity subdynamics stabilization.

$$\dot{e}_2 = -a_1 x_1 - \beta x_2 + a_2 x_3 + f_1 + k_1 x_2 \quad (23)$$

For the effect of the phase transformation on the actuator dynamics, we propose the following dissipation function.

$$L_1 = \frac{d}{dt}\sum_{i=1}^{2}\left(\frac{1}{2}e_i^2\right) + \frac{1}{2}(\|\boldsymbol{h}\|^2 - \mu^2 f_1^2) \quad (24)$$

where $\boldsymbol{h} = [p_1 x_1 \quad p_2 x_2]^T$ is the output vector and $\mu \in \mathbb{R}^+$. Substituting (16) and (18) into (19) gives

$$\begin{aligned} L_1 = {} & [e_1 x_2 + e_2(-a_1 x_1 - \beta x_2 + a_2 x_3 + f_1 + k_1 x_2)] \\ & + \frac{1}{2}(p_1^2 x_1^2 + p_2^2 x_2^2 - \mu^2 f_1^2) \end{aligned} \quad (25)$$

One can write (23) as follows:

$$\begin{aligned} L_1 = {} & -\alpha_1 e_1^{2\cdot} - \frac{1}{2}\left(\mu f_1 - \frac{e_2}{\mu}\right)^2 - \frac{1}{4}\mu^2 f_1^2 \\ & + e_2[\alpha_2 x_1 + (-\beta + \alpha_3)x_2 + a_2 x_3] \end{aligned} \quad (26)$$

with

$$\alpha_1 = k_1 - \frac{1}{2}p_2^2 k_1^2 - \frac{1}{2}p_1^2, \quad \alpha_2 = k_1\left(\frac{1}{\mu^2} - \frac{1}{2}p_2^2\right) + 1 - a_1, \quad \alpha_3 = k_1 + \frac{1}{2}p_2^2 + \frac{1}{\mu^2}$$

To satisfy the dissipation condition for the function f_1, a virtual control x_3^* is chosen as follows

$$x_3^* = \frac{-\alpha_2 x_1 - (\hat{\beta} + \rho + \alpha_3)x_2}{a_2} \quad (27)$$

where $\hat{\beta}$ is the estimation of β to be provided by the adaptive law and ρ is a smooth function to be designed later. Substituting (26) into (27), the function F_1 becomes

$$\begin{aligned} L_1 = {} & -\alpha_1 e_1^{2\cdot} - \frac{1}{2}\left(\mu f_1 - \frac{e_2}{\mu}\right)^2 - \frac{1}{4}\mu^2 f_1^2 \\ & - e_2\, x_2\,(\hat{\beta} - \beta + \rho) \end{aligned} \quad (28)$$

It follows that the condition $F_1 < 0$ is satisfied only if

$$\hat{\beta} - \beta + \rho > 0 \quad (29)$$

Step 3: Real control law

The real control input to system in (11) is designed to ensure the dissipation condition in (13). Thus, a new function F_2 is constructed as follows

$$L_2 = \frac{d}{dt}\sum_{i=1}^{3}\left(\frac{1}{2}e_i^2\right) + \frac{1}{2}\left(\|\boldsymbol{h}\|^2 - \mu^2\sum_{i=1}^{2}(f_i^2)\right) \quad (30)$$

With $e_3 = x_3 - x_3^*$, one can obtain

$$\begin{aligned} \dot{e}_3 = {} & -b_1(x_3 - T_0) + b_2 u \\ & + f_2 - \left[\frac{\alpha_2\dot{x}_1 - (\hat{\beta} + \rho + \alpha_3)\dot{x}_2 - \left(\dot{\hat{\beta}} + \dot{\rho}\right)x_2}{a_2}\right] \end{aligned} \quad (31)$$

It follows that

$$\begin{aligned} L_2 = {} & -\alpha_1 e_1^{2\cdot} - \frac{1}{2}\left(\mu f_1 - \frac{e_2}{\mu}\right)^2 - \frac{1}{4}\mu^2 f_1^2 - e_2\, x_2\,(\hat{\beta} - \beta + \rho) \\ & e_3\left(-b_1(x_3 - T_0) + b_2 u + f_2 - \left[\frac{\alpha_2\dot{x}_1 - (\hat{\beta} + \rho + \alpha_3)\dot{x}_2 - \left(\dot{\hat{\beta}} + \dot{\rho}\right)x_2}{a_2}\right]\right) \end{aligned} \quad (32)$$

The real control law for system in (11) is obtained as follows

$$u = \frac{1}{b_3}\left[b_1(x_3 - T_0) + \frac{\alpha_2\dot{x}_1 - (\hat{\beta} + \rho + \alpha_3)\dot{x}_2 - \left(\dot{\hat{\beta}} + \dot{\rho}\right)x_2}{a_2}\right] \quad (33)$$

C. Stability Analysis

To address the global stability of the SMA actuator, the dynamic model in (11) is put in an error form using the definitions (21), (23), and (30).

$$\begin{cases} \dot{e}_1 = e_2 + k_1\, e_1 \\ \dot{e}_2 = -a_1 x_1 - \beta x_2 + a_2 x_3 + f_1 + k_1(e_2 - k_1\, e_1) \\ \dot{e}_3 = (b_1 x_2(x_3 - T_0) + b_2 u + f_2 \\ \quad - \left[\dfrac{\alpha_2\dot{x}_1 - \left(\hat{\beta} + \rho + \alpha_3\right)\dot{x}_2 - \left(\dot{\hat{\beta}} + \dot{\rho}\right)x_2}{a_2}\right]\right) \end{cases} \quad (34)$$

Consider a Lyapunov candidate function $V = \sum_{i=1}^{3}\left(\frac{1}{2}e_i^2\right)$, the function L_2 given in (30) can be written as follows.

$$L_2 = \dot{V} + \frac{1}{2}\left(\|\boldsymbol{h}\|^2 - \mu^2\sum_{i=1}^{2}(f_i^2)\right) \quad (35)$$

From (33), it follows that $L_2 \leq 0$ if and only if $\lim_{t\to\infty}(\hat{\beta} - \beta + \rho)$, thus.

$$\dot{V} \leq -\frac{1}{2}\left(\|\boldsymbol{h}\|^2 - \mu^2\sum_{i=1}^{2}(f_i^2)\right) \quad (36)$$

The integration of (36) for the case of $f_1 = f_2 = 0$ gives

$$V(t) \leq V(0) - \frac{1}{2}\int_0^t \|\boldsymbol{h}(\boldsymbol{t})\|^2\, dt \leq V(0) \quad (37)$$

It can be seen from system in (35), that the origin ($e_1 = e_2 = e_3 = 0$) is globally stable. For the case of non-parametric uncertainties where $f_1 \neq 0, f_2 \neq 0$, the following semi-defined function is considered

$$W(\boldsymbol{e},\boldsymbol{f}) = -\alpha_1 e_1^2 - \frac{1}{2}\left(\mu f_1 - \frac{e_2}{\mu}\right)^2 - \frac{1}{2}\left(\mu f_2 - \frac{e_3}{\mu}\right)^2 - \left(\frac{1}{2}\mu f_1 - \frac{(\alpha_2 + \hat{\beta} + \rho)e_3}{\mu a_3}\right)^2 - \left(e_2 - \frac{(\alpha_2 + \hat{\beta} + \rho)e_3}{\mu a_3}\right)^2 \varphi\, x_2 \quad (38)$$

From (35), it follows that

$$\dot{V} \leq -W(\boldsymbol{e},\boldsymbol{f}) \leq 0 \quad (39)$$

According to Lasalle-Yoshizawa theorem [26], all solutions of (11) are globally uniformly asymptotically stable and satisfy the following condition $\lim_{t\to\infty} W = 0$.

D. SMA-based Array Actuator

Consider the case of an array actuator where all the individual actuators are connected to the power supply source. The following distributed heat law is considered for thermal activation of the i^{th} SMA actuator.

$$u_i = \frac{1}{b_3}\left[b_1(x_{3,i} - T_0) + \frac{\alpha_2 \dot{x}_{1,i} - (\hat{\beta} + \rho + \alpha_3)\dot{x}_{2,i} - \left(\dot{\hat{\beta}} + \dot{\rho}\right) x_{2,i}}{a_2}\right] \quad (40)$$
$$k\left[\sum_{j\in\mathcal{N}} a_{ij}(\boldsymbol{x}_i - \boldsymbol{x}_j) + a_{i0}(\boldsymbol{x}_i - \boldsymbol{x}_d)\right] +$$

with $k \in \mathbb{R}^+$ is a control gain.

The control objective is achieved when all the actuators' states reach the desired value according to the following consensus

$$\left\{ \lim_{t\to t_s} \|\boldsymbol{x}_i - \boldsymbol{x}_d\|_2 = 0 \right. \quad (41)$$

where, t_s is the settling time and a_{ij} are the coefficients of the adjacency matrix of the activation topology.

IV. Numerical Results

To demonstrate the efficacy of the theoretical developments, numerical calculations have been performed. Since the twist angle θ measures the actuating capability of the SMA rotary actuator, two desired twist angle paths are considered. First, the SMA wire is heated to its final austinite temperature A_f to achieve the desired steady angle $\theta_t = 100°$. The SMA actuator was then heated between A_s and A_f to track a desired time-varying sinusoidal twist angle in the presence of external disturbances. The non-parametric uncertainties f_1 and f_2 are determined as follows:

$$\begin{cases} f_1 = ae^{b(T-T_0)}\sin(\xi) \\ f_2 = ae^{b(T-T_0)}\cos(\xi) \end{cases}$$

with $a = 1e-7, b = 0.25$.

The thermomechanical properties of the selected $NiTi$ material and the actuator parameters used in this simulation are shown in Table I.

TABLE I. NiTi Material and Actuator Properties

NiTi material		Actuator wire	
property	Value	property	Value
M_s ,M_f (°C)	18.4, 9	$\rho\ (kg/m^{3\cdot})$	6450
A_s , A_f (°C)	34.5, 49	$C_p\ (J/Kg°C)$	2046
C_m , C_a $(Pa/°C)$	8e6, 13.8e6	$d\ (mm)$	1.0
$\sigma_{s_{cr}}$, $\sigma_{a_{cr}}$ (Pa)	100e6,100e6	$L_0\ (mm)$	100
α_s , α_f	1.1e-6, 6.6e-6	$R(\Omega)$	3.0
ϵ_L	0.067	$T_0\ (°C)$	25

Scenario 1: A simulation of angle-temperature actuation was run to validate the single actuator control law (33). The twist angle achieved the desired $\theta_t = 100°C$ without overshooting, the temperature T saturated around $70°C$ and the equivalent stress σ reached $600\ MPa$. Fig. 2 shows the simulation results for with tuning of parameter μ.

Fig. 3 demonstrates that when the suggested HARC method is applied, the transient response of the actuator states converges faster and without oscillation compared to other conventional adaptive backstepping control (CABC) methods.

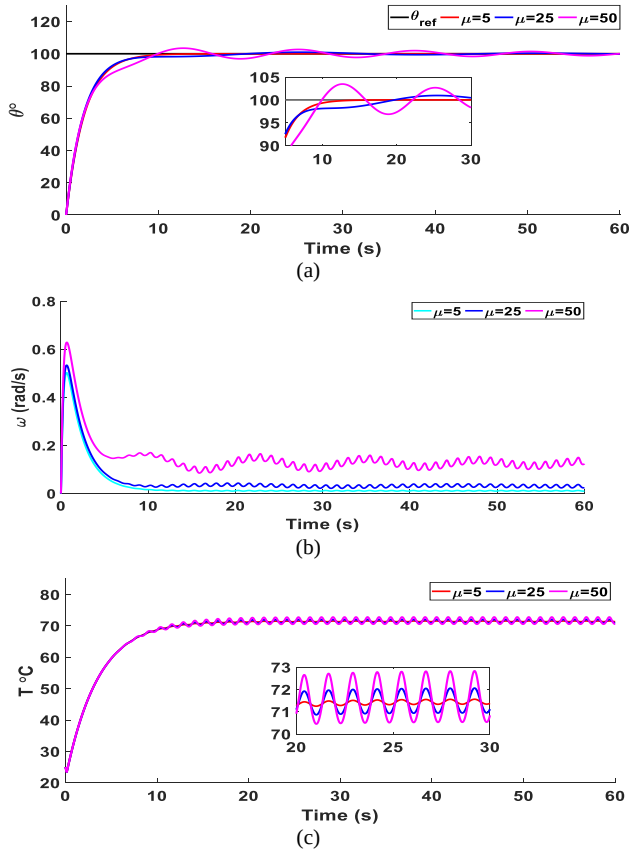

Fig. 2. Actuator transient response with tuning of parameter μ: a) Twist angle θ, b) rotary velocity ω, and c) heating temperature T.

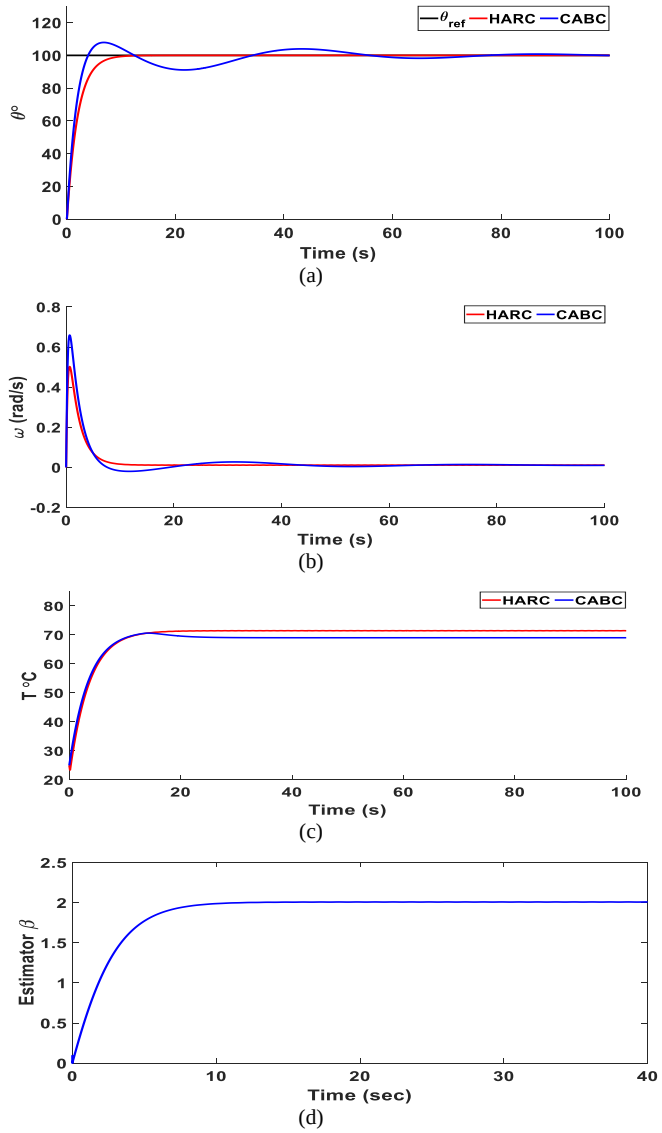

Fig. 3. Comparison between proposed HARC and CABC methods: (a) Twist angle θ, (b) rotary velocity ω, and (c) heating temperature T, d) parametric estimator β.

Scenario 2: To simulate the cooperative actuation of an array SMA actuator to overcome individual actuator load bearing limitation, a cooperative task is attributed to a set of four actuators to track a sinusoidal twist angle $\theta_t(t) = 60sin(0.5t)(°)$. The actuators were put under initial conditions of temperature $T = [\ 25\ \ 50\ \ 65\ \ 80]^{\circ}C$ and initial twist angle $\theta = [-20\ \ -60\ \ 60\ \ 120]^{\circ}$. A disturbance of $\Delta T = 5°C$ is introduced at $t = 20\ s$ simulating a sudden change in the electrical current and checking the controller's robustness.

The four actuators were actuated according to activation topology shown in Fig. 4. The distributed control law in (41) is used to activate the array controller and the results are shown in Fig. 5.

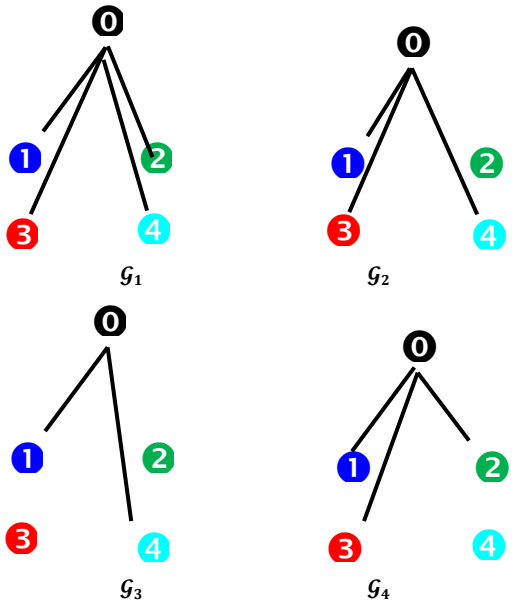

Fig. 4. Actuation topology for a four-SMA actuator.

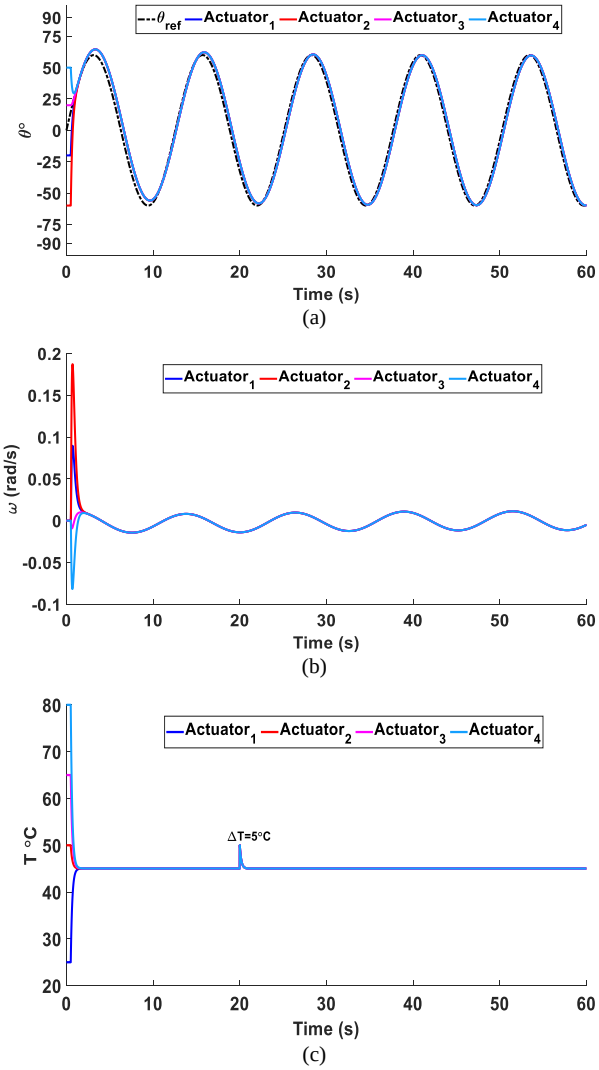

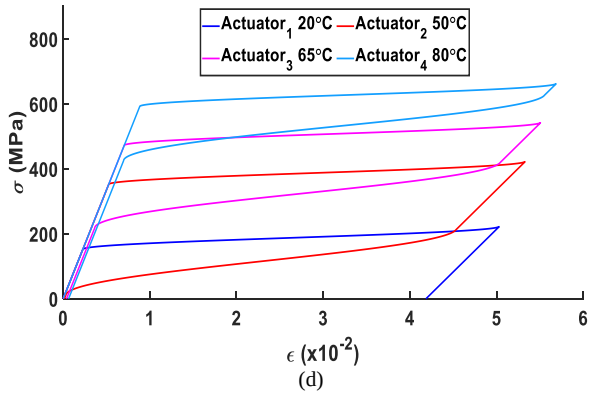

(d)

Fig. 5. Simulation results for a multi-SMA actuator under time-varying actuation topology: a) twist angle, b) angular speed, c) temperature, and d) stress-strain diagram.

Remark 1: Fig. 3 shows a fair comparison between the proposed hybrid adaptive robust control scheme and one of the conventional backstepping control approaches. The comparison shows that the hybrid approach provide high-performance and more stable transient response rather than the conventional solution that ignores the nonlinear effect of the system parameters.

Remark 1: Fig. 3(d) shows that the parameter estimator $\hat{\theta}(t)$ starting from the initial condition $\hat{\theta}(0) = 0$ converges to its steady-state value $\theta_{ss} = 2$ without oscillation.

Remark 2: Changing the design parameter μ in (24), the transient response of the twist angle, angular speed, and temperature states are affected as shown in Figure 4. The tuning of the parameter μ directly affects the convergence of the actuator states. Short settling time, small fluctuations, and stable response are obtained with small values of μ.

V. Conclusion

This paper proposed a hybrid adaptive robust control approach for thermal activation of a multi-SMA rotary actuator in the presence of parametric and non-parametric uncertainties using adaptive backstepping control. First, a control method that integrates adaptive immersion and invariance (I&I adaptive) control, L_2-gain control, a parameter estimation law, and asymptotic smooth disturbance functions for induced effect of SMA phase transformation was developed. Pre-defined target system and PDEs solving process, presented in the conventional adaptive backstepping methods, were skipped altogether. Then, the developed control scheme was extended to actuate a multi-agent or array controller where a cluster of controllers are used together to cooperate for load bearing beyond their individual capabilities. The distributed control protocols were designed to work in coordination under switching activation topology to avoid excessive current supply and minimize the activation cost. Different simulation scenarios for tracking the target twist angle, thermal load disturbance, and parameter tuning have been carried out to demonstrate the effectiveness of the suggested control method. From what can be seen in simulation results, the suggested hybrid adaptive robust control method offers a viable solution for improving the performance of SMA actuators mainly in terms of stability and robustness. Future works will consider the trade-off between actuator performance and parameter tuning and will extend the proposed control method to other types of SMA controllers.

Acknowledgment

This project was funded by the Deanship of Scientific Research (DSR), King Abdulaziz University, Jeddah, under grant No. (G-1436-135-510). The authors, therefore, acknowledge with thanks DSR technical and financial support.

References

[1] S. K. Yadav, Shape Memory Alloy Actuators: A Review, Int. J. Res. Appl. Sci. Eng. Technol., 7 (5) (2019) 799–802. doi: 10.22214/ijraset.2019.5134.

[2] T. Devashena and K. Dhanalakshmi, Simultaneous Measurements in Shape Memory Alloy Springs to Enable Structural Health Monitoring by Self-Sensing Actuation, Arabian Journal for Science and Engineering, 46 (2021) 6015-6025.

[3] D. K. Soother, J. Daudpoto, and B. S. Chowdhry, Challenges for practical applications of shape memory alloy actuators, Mater. Res. Express, vol. 7 (7) (2020). doi: 10.1088/2053-1591/aba403.

[4] H. Yuan, J. C. Fauroux, F. Chapelle, and X. Balandraud, A review of rotary actuators based on shape memory alloys, J. Intell. Mater. Syst. Struct., 28 (14) (2017) 1863–1885. doi: 10.1177/1045389X16682848.

[5] M. Sansone, S. Ameduri, A. Concilio, and E. Cestino, Understanding Shape Memory Alloy Torsional Actuators: From the Conceptual to the Preliminary Design," Actuators, vol. 11, no. 3, pp. 1–25, 2022. doi: 10.3390/act11030081.

[6] N. Simiriotis, M. Fragiadakis, J. F. Rouchon, and M. Braza, Shape control and design of aeronautical configurations using shape memory alloy actuators, Comput. Struct., 244 (2021). doi: 10.1016/j.compstruc.2020.106434.

[7] K. Hu, K. Rabenorosoa, and M. Ouisse, A Review of SMA-Based Actuators for Bidirectional Rotational Motion: Application to Origami Robots, Front. Robot. AI, 8 (2021) 1–21. doi: 10.3389/frobt.2021.678486.

[8] D. J. S. Ruth, J. W. Sohn, K. Dhanalakshmi, and S. B. Choi, Control Aspects of Shape Memory Alloys in Robotics Applications: A Review over the Last Decade, Sensors, 22 (13) (2022) 1–17. doi: 10.3390/s22134860.

[9] A. El Naggar and M. A. Youssef, Shape memory alloy heat activation: State of the art review, AIMS Mater. Sci., 7 (6) (2020) 836–858, 2020. doi: 10.3934/matersci.2020.6.836.

[10] J. S. Owusu-DanquahA. F. Saleeb, On the modeling of the effect of processing and heat treatment on actuation behaviors of high temperature ternary and quaternary shape memory alloys, J. Alloys Compd., 714 (2015) 493–501.

[11] J. Guo, C. Zhao, and Z. Song, Discussion on research status and key technologies of morphing aircraft, J. Phys. Conf. Ser., 2228 (1) 2022. doi: 10.1088/1742-6596/2228/1/012021.

[12] S. Karmakar, V. Gaddam, J. Kim, A. K. Mishra, and A. Sarkar, Helical SMA Actuator based Artificial Muscle and Arm with Sliding Mode Control, ACM Int. Conf. Proceeding Ser., (2021) 1–5. doi: 10.1145/3478586.3480722.

[13] N. Keshtkar, S. Keshtkar, and A. Poznyak, Deflection sliding mode control of a flexible bar using a shape memory alloy actuator with an uncertainty model, Appl. Sci., 10 (2) (2020). doi: 10.3390/app10020471.

[14] F. O. M. Joseph and T. Podder, "Sliding mode control of a shape memory alloy actuated active flexible needle," Robotica, 36, (8) (2018) 1188–1205. doi: 10.1017/S0263574718000334.

[15] R. Hmede, F. Chapelle, and Y. Lapusta, Review of Neural Network Modeling of Shape Memory Alloys, Sensors, 22 (15) (2022). doi: 10.3390/s22155610.

[16] A. Mendizabal, P. Márquez-Neila, and S. Cotin, Simulation of hyperelastic materials in real-time using deep learning, Med. Image

Anal., 59 (2020) 1–11. doi: 10.1016/j.media.2019.101569.

[17] J. S. Owusu-Danquah, A. Bseiso, and S. Allena, Artificial neural network models to predict the response of 55NiTi shape memory alloy under stress and thermal cycles, Neural Computing and Applications, 34 (5) (2022). 3829–3842. doi: 10.1007/s00521-021-06643-x.

[18] A. Gómez-Espinos, R. C. Sundin, I. L. Eguren, E. Cuan-Urquiz, and C. D. Treviño-Quintanilla, Neural network direct control with online learning for shape memory alloy manipulators, Sensors, 19(11) (2019) 1–17. doi: 10.3390/s19112576.

[19] R. E. Precup, C. A. Bojan-Dragos, E. L. Hedrea, R. C. Roman, and E. M. Petriu, Evolving Fuzzy Models of Shape Memory Alloy Wire Actuators, Rom. J. Inf. Sci. Technol., 24 (4) (2021) 353–365.

[20] K. Suwat, Adaptive Fuzzy Sliding-Mode Position Control of a Shape Memory Alloy Actuated System. Applied Mechanics and Materials, vol. 789–790, Trans Tech Publications, Ltd., (2015) 946–950.

[21] L. Su and X. Zhao, Prescribed Adaptive Backstepping Control of Nonlinear Systems Preceded by Hysteresis in Piezoelectric Actuators, Int. J. Precis. Eng. Manuf. 23 (2022) 733-740.

[22] A. M. Khan, B. Shin, M. Usman, and Y. Kim, Backstepping control of novel arc-shaped SMA actuator, Microsyst. Technol., 28 (10) (2022) 2191–2202. doi: 10.1007/s00542-022-05250-7.

[23] J. M. Jani, S. Huang, M. Leary, and A. Subic, Numerical modeling of shape memory alloy linear actuator, Comput. Mech., 56 (3) (2015) 443–461. doi: 10.1007/s00466-015-1180-z.

[24] W. Wang, Y Xiang, J Yu, L Yang, Development and Prospect of Smart Materials and Structures for Aerospace Sensing Systems and Applications. Sensors (Basel). 23(3) (2023) 1545. doi: 10.3390/s23031545.

[25] M. H. Elahinia and M. Ahmadian, An enhanced SMA phenomenological model: I. The shortcomings of the existing models, Smart Mater. Struct., 14 (6) (2005) 1297–1308. doi: 10.1088/0964-1726/14/6/022.

[26] C. Liang and C. A. Rogers, One-Dimensional Thermomechanical Constitutive Relations for Shape Memory Materials, J. Intell. Mater. Syst. Struct., 1 (2) (1990) 207–234. doi: 10.1177/1045389X9000100205.

[27] D. Karagiannis and A. Astolfi, Nonlinear adaptive control of systems in feedback form: An alternative to adaptive backstepping, Syst. Control Lett., 57 (9) (2008) 733–739, 2008. doi: 10.1016/j.sysconle.2008.02.006.